


Two Molecular Weights Holothurian Glycosaminoglycan and Hematoporphyrin Derivative-Photodynamic Therapy Inhibit Proliferation and Promote Apoptosis of Human Lung Adenocarcinoma Cells

Integrative Cancer Therapies
Volume 22: 1–8
© The Author(s) 2023
Article reuse guidelines:
sagepub.com/journals-permissions
DOI: 10.1177/15347354221144310
journals.sagepub.com/home/ict


Dai Hao-Yu, MM^{1*} , Yu Ding-Yi, MM^{1*}, Xiao Bao-Hong, MM¹, Sui Aihua, MM¹, Ding Xiao-Qian, MM¹, and Lin Cun-Zhi, MD¹

Abstract

Holothurian glycosaminoglycan (hGAG) is extracted from the body wall of the sea cucumber, and previous studies have shown many unique bioactivities of hGAG, including antitumor, anti-angiogenesis, anti coagulation, anti thrombosis, anti-inflammation, antidiabetic effect, antiviral, and immune regulation. The effects of 3W and 5W molecular weights hGAG with hematoporphyrin derivative-photodynamic therapy (HPD-PDT) on lung cancer were investigated. Human lung adenocarcinoma A549 cells were divided into 6 groups: control group, 3W molecular weight hGAG group, 5W molecular weight hGAG group, HPD-PDT group, 3W molecular weight hGAG + HPD-PDT group, and 5W molecular weight hGAG + HPD-PDT group. Cell morphology was observed under inverted phase contrast microscope. Cell proliferative activity was detected by CCK8 and cell apoptosis was assayed by Hoechst33258 staining and flow cytometry. The results showed that two different molecular weights hGAG could inhibit proliferation, promote apoptosis rates of A549 cells, and enhance the sensitivity of A549 cells to HPD-PDT. The combined use of hGAG and HPD-PDT has synergistic inhibitory effects on A549 cells, and the effects of 3W molecular weight hGAG are better than that of 5W molecular weight hGAG.

Keywords

holothurian glycosaminoglycan, hGAG, HPD-PDT, apoptosis, lung cancer

Submitted July 10, 2022; revised October 23, 2022; accepted November 23, 2022

Introduction

Lung cancer, the second most commonly malignant tumors, caused 2.20 million new diagnoses and 1.79 million tumor-related deaths in 2020, and the latter accounts for about 18% of total cancer mortality.¹ The survival rate of patients with lung cancer after 5 years was only 10% to 20% in most countries, including China.²⁻⁴ In China, it was estimated that there were 0.81 million new lung cancer cases in 2020, 0.54 million in men, accounting for 38% of global new lung cancer cases in males, and 0.27 million in women, accounting for 36% of global new lung cancer cases in females.⁵ In histopathological classification, lung cancer consists of 2 main types, non-small cell lung cancer (NSCLC) and small cell lung cancer (SCLC), and the proportion of the former is more than 85%.^{6,7} In NSCLC, adenocarcinoma is the most prevalent subtype, accounting for approximately 40% of lung cancer's new diagnoses.⁸

Sea cucumber is of high pharmacological value, and there are many kinds of active components existing in the sea cucumber. Sea cucumber polysaccharide is a kind of acidic mucopolysaccharide, which is extracted from the body wall of the sea cucumber and includes 2 main subtypes: one is holothurian glycosaminoglycan (hGAG) and the other is sea cucumber fucoidan.⁹ With deep analysis of the structure and bioactivities of hGAG, the content of sulfate groups, the position of sulfation and molecular weight

¹The Affiliated Hospital of Qingdao University, Qingdao, Shandong, China

*These authors contributed equally to this work and should be considered co-first authors.

Corresponding Author:

Lin Cun-Zhi, Department of Respiratory and Critical Care Medicine, The Affiliated Hospital of Qingdao University, Qingdao 266003, Shandong, China.
Email: lindoc@126.com



may predominantly determine the bioactivities of hGAG.^{10,11} Nowadays, many unique biological activities of hGAG have been discovered, such as antitumor, anti-angiogenesis,¹² anti coagulation,^{11,13} anti thrombosis,¹⁴ anti inflammation,¹⁵ antidiabetic effect,¹⁶ antiviral,¹⁷ and immune regulation.¹⁸ Moreover, a previous study of our research group has confirmed that hGAG can strengthen the sensitivities of tumor cells to chemotherapy.¹⁹

Photodynamic therapy (PDT) is also called photoradiation therapy or photochemical therapy, and now is becoming a new form of tumor treatment. It encompasses 3 important parts: photosensitizer, laser with appropriate wavelength and oxygen in tumor cells.²⁰ The process of PDT for cancer treatment is as follows: tumor cells selectively ingest photosensitizers, and then laser irradiation triggers the photochemical reaction that leads to tumor cell apoptosis and necrosis via reactive oxygen species (ROS), while normal tissues or organs are less affected. Nowadays, the most prevalent kind of photosensitizers is hematoporphyrin in clinical practice.²¹ Previous studies indicated that PDT combined with chemotherapy, target therapy, and immune therapy could gain better curative effectiveness in patients with tumor.²²⁻²⁴ However, it is still not known that whether hGAG could enhance the sensitivity of tumor cells to HPD-PDT or not. Based on the previous research results, this study was performed to explore the combined effects of 3W and 5W molecular weights hGAG and photodynamic therapy on inhibiting proliferation and promoting apoptosis in A549 cells, and explore whether there were differences in antitumor effects of sea cucumber polysaccharides with 3W and 5W molecular weights.

Material and Methods

Substances

Herein, 3W and 5W molecular weights sea cucumber polysaccharide was isolated and purified by Ocean University of China. The structure of the monosaccharide is as shown in Figure 1, and 3W and 5W molecular weights hGAG are polymers consisting of different amounts of monosaccharides.

Cell Culture

The human lung adeno carcinoma cell line A549 was provided by the Central Laboratory of the Affiliated Hospital of Qingdao University. The cells were cultured in complete medium which consisted of 10% heat-inactivated fetal bovine serum (HyClone), 1% penicillin-streptomycin (100 U/ml penicillin and 100 U/ml streptomycin; Servicebio), and 89% DMEM high-glucose medium (HyClone) at 37°C in humidified 5% CO₂. All experiments were performed when cells grew to 80% to 90% confluence.

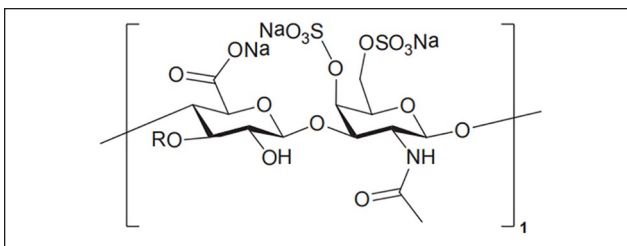


Figure 1. Chemical structure of hGAG monosaccharide.

CCK8 Detection

Cell viability was assessed by CCK8 (Beyotime Institute of Biotechnology, Shanghai, China). A549 cells were seeded in 96-well plates at a density of 1×10^4 cells/well. A proper amount of complete culture medium was added into each well, and cells were incubated for 24 hours. As for the concentration of hGAG, we referred to our previous study,¹⁹ in which it was found that concentration at 100 µg/ml of 3W and 5W hGAG did not show any cytotoxicity to the cancer cells and showed the most obvious effect compared with other concentrations. Cells were divided into 6 groups: control group; 3W molecular weight hGAG therapy group (the concentration of hGAG was 100 µg/ml); 5W molecular weight hGAG group (the concentration of hGAG was 100 µg/ml); HPD-PDT group (hematoporphyrin derivative concentration was 8 µg/ml and cells were irradiated by a 630 nm laser; in the process, the laser energy density was 50 mW/cm², the spot diameter was about 9 cm, the irradiation time was 2 minutes and the vertical distance between the emitter and the 96-well plate was 9 cm.); 3W molecular weight hGAG combined with photodynamic therapy group (the concentration of hGAG was 100 µg/ml; after incubated for 24 hours and washed with PBS, the remaining treatment was the same as HPD-PDT group); 5W molecular weight hGAG combined with photodynamic therapy group (the concentration of hGAG was 100 µg/ml and the treatment was the same as 3W hGAG + HPD-PDT group). Each group included 3 wells, washed with 100 µl phosphate-buffered saline (PBS) and observed by inverted phase contrast microscope (Olympus, China). We added 10 µl CCK8 + 90 µl complete medium into each group and cultured A549 cells at 37°C. A microplate reader was used to measure the optical density (OD) at 450 nm after 30 minutes. The cell viability ratio was calculated as follows: Cell survival ratio (%) = $(OD_2 - OD_0) / (OD_1 - OD_0) \times 100\%$. OD₂ is the absorbance of the experimental group, OD₁ is the absorbance of the control group, and OD₀ is the absorbance of the blank control group. The coefficient of drug interaction (CDI) was utilized to evaluate the inhibitory effects of the combinations. The formula to calculate CDI is as follows: $CDI = AB / (A \times B)$. According to the absorbance of each group, AB is the ratio of the combination group to the control group, and

A or B is the ratio of the non-combination group to the control group. According to CDI, if the CDI value is <1 , it indicates there is synergism between hGAG and HPD-PDT; especially if the CDI value is <0.7 , hGAG and HPD-PDT are significantly synergistic; if the CDI value is $=1$, hGAG and HPD-PDT are additive; if the CDI value is >1 , there is antagonism between hGAG and HPD-PDT.

Hoechst33258 Staining

A549 cells were inoculated in 24-well plates, divided into 6 groups and treated with various concentrations of agents as described above. The culture medium was removed after 48 hours treatment. 0.5 ml cell fixative was added to each well and cells were fixed for 15 minutes. After washing twice using PBS, 0.5 ml Hoechst staining solution (Beyotime Institute of Biotechnology, Shanghai, China) was added into each well. After 5 minutes of staining, we removed the staining solution and washed again twice with PBS. An inverted fluorescence microscope (Olympus, China) was used for observation.

Flow Cytometric Analysis of Apoptosis

Apoptotic cells in the early stage and the late stage can bond with Annexin V-FITC and propidium iodide (PI), respectively, and Annexin V-FITC/PI double-staining could be used to distinguish early and late apoptotic cells. After being treated for 48 hours and washed with PBS, A549 cells were centrifuged for 5 minutes (1000 rpm) and washed twice with PBS, and then mixed with 5 μ l Annexin V-FITC and 10 μ l PI. After incubation at room temperature for 10 minutes, a flow cytometer (BD Biosciences, Franklin Lakes, NJ) was used to analyze the apoptosis of A549 cells.

Statistical Analysis

All experiments were repeated at least 3 times. SPSS statistical software, version 26.0 (SPSS Inc, IBM, Chicago, IL) was used for data analysis, and the numerical variables were expressed as mean \pm standard deviation ($X \pm S$). All groups were tested for homogeneity of variance before comparison. One-way analysis of variance was used to compare the mean between groups. LSD- t (least significant different- t) test was used for pairwise comparison, with the level of the test $\alpha = .05$, that is, when the value of P is $< .05$, the difference was statistically significant.

Results

Morphology of A549 Cells Line

The morphological changes of the A549 cells line were observed under inverted phase contrast microscope. It showed that A549 cells in the control group were in a good

state and arranged closely, with a large number and small intercellular space. Cells were flat and grew adherently. There were clear nucleoli, full cell body, and transparent cytoplasm. In contrast, after hGAG and HPD-PDT treatment, the cell count in the culture medium decreased; the cells were sparse and less dense; the cell body protrusions got shorter; the cellular volume became smaller, and some necrotic cells were visible, among which the 2 combination groups were the most obvious. Compared with 5W hGAG group, the morphological changes of the cells in 3W hGAG group were more obvious (Figure 2).

The Inhibition Effects of hGAG and HPD-PDT on A549 Cell Line

To reveal the effects of hGAG and HPD-PDT on cell viability, CCK8 assay was performed. The OD value and proliferative activity of A549 cells were measured (Table 1). It was observed that 3W and 5W molecular weights hGAG and HPD-PDT exhibited inhibitory effects on the proliferation of A549 cells ($P < .05$). And hGAG could promote the proliferation inhibition of A549 cells by HPD-PDT and enhance the sensitivity of HPD-PDT ($P < .05$). Especially the inhibitory effect of 3W molecular weight hGAG was more clear than that of 5W molecular weight hGAG ($P < .05$). CDI values of the 2 molecular weights of hGAG and photodynamic combination were 0.894 (3W) and 0.933 (5W), respectively, which showed that synergistic effects could be obtained when hGAG and HPD-PDT are applied together.

The Apoptosis Effects of hGAG and HPD-PDT on A549 Cells

Apoptotic A549 cells were detected by Hoechst33258 staining. There were no obvious apoptotic cells in the control group, while shrunken, hyperchromatic, and pyknotic cells and nuclear fragmentation could be observed under microscope in experimental groups. (Figure 3). And we observed lower cell count and less cell density and more obvious apoptotic cells in the 3W molecular weight hGAG group than in the 5W molecular weight hGAG group. The 2 combination groups were the most obvious with the lowest cell count and the least cell density. The results of total apoptosis rates of A549 cells from flow cytometric analysis also showed that apoptosis rates in experimental groups significantly increased compared with the control group and the apoptosis rates in each combination group were the highest compared with the single drug group ($P < .05$). It indicated that 3W and 5W molecular weights hGAG and HPD-PDT could induce the apoptosis of A549 cells and hGAG increased the apoptosis rates induced by HPD-PDT ($P < .05$). The apoptosis effect of 3W molecular weight hGAG was more obvious than that of 5W molecular weight hGAG ($P < 0.05$; Table 2 and Figures 3 and 4).

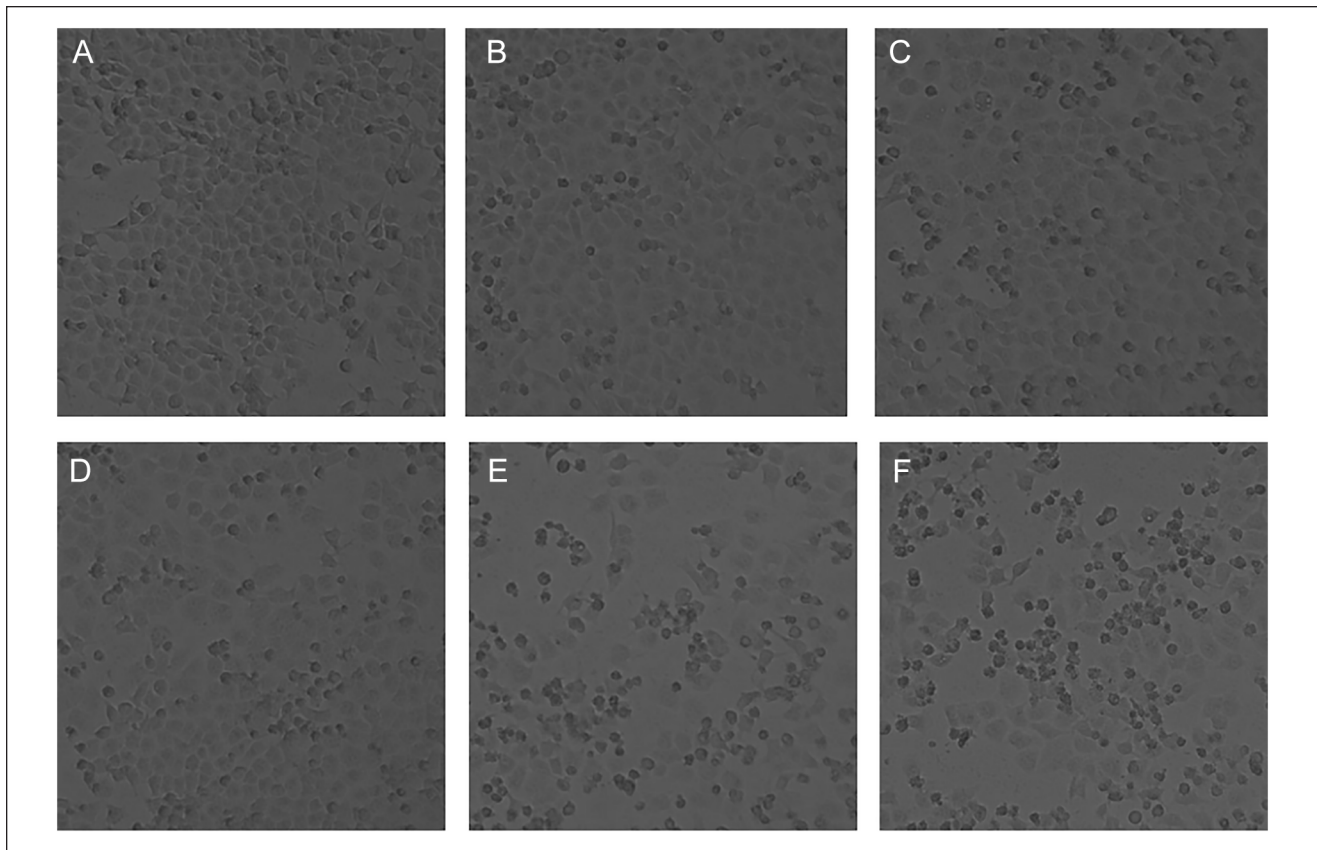


Figure 2. Observation of A549 cells showed sparse and less dense cells, decreased cell count, short cell body protrusions, small cellular volume, and some necrotic cells in experimental groups compared with the control group. ($\times 10$) (A) Control group. (B) 3W hGAG group. (C) 5W hGAG group. (D) HPD-PDT group. (E) 3W hGAG + HPD-PDT group. (F) 5W hGAG + HPD-PDT group.

Table 1. The OD Value and Proliferative Activities in Different Groups (Mean \pm SD, $n=3$).

Groups	OD value	SR (%)
Control	1.852 \pm 0.015	100.000 \pm 1.181
3W hGAG**	1.469 \pm 0.021	77.351 \pm 2.786
5W hGAG*	1.539 \pm 0.017	81.535 \pm 3.732
HPD-PDT*	1.354 \pm 0.037	70.558 \pm 4.445
3W hGAG + HPD-PDT###	0.961 \pm 0.052	47.332 \pm 7.553
5W hGAG + HPD-PDT**	1.049 \pm 0.034	52.541 \pm 3.894

Abbreviations: OD, optical density; SR, survival ratio; hGAG, holothurian glycosaminoglycan; HPD-PDT, hematoporphyrin derivative-photodynamic therapy.

* $P < .05$ compared with the control group.

** $P < .05$ compared with the 5W hGAG group.

*** $P < .05$ compared with the HPD-PDT group.

$P < .05$ compared with 5W hGAG + HPD-PDT group. The SR was most obvious in 3W hGAG + HPD-PDT group. $P < .05$ was considered statistically significant.

Discussion

Worldwide, the morbidity and mortality of lung cancer rank first in males, while in females cancer deaths rank third, after breast cancer and colorectal cancer and new cases rank second, after breast cancer.¹ Lung cancer has become a heavy burden for China.²⁵ With the implementation of

low-dose CT screening, more and more patients at early stages have been discovered and a significant decrease has been gained in mortality.²⁶ In the meantime, with the development of chemotherapy, target therapy, and immune therapy, the overall survival and disease-free survival have greatly progressed.²⁷ However, the limitations of these treatments are also assignable. Radiochemotherapy can

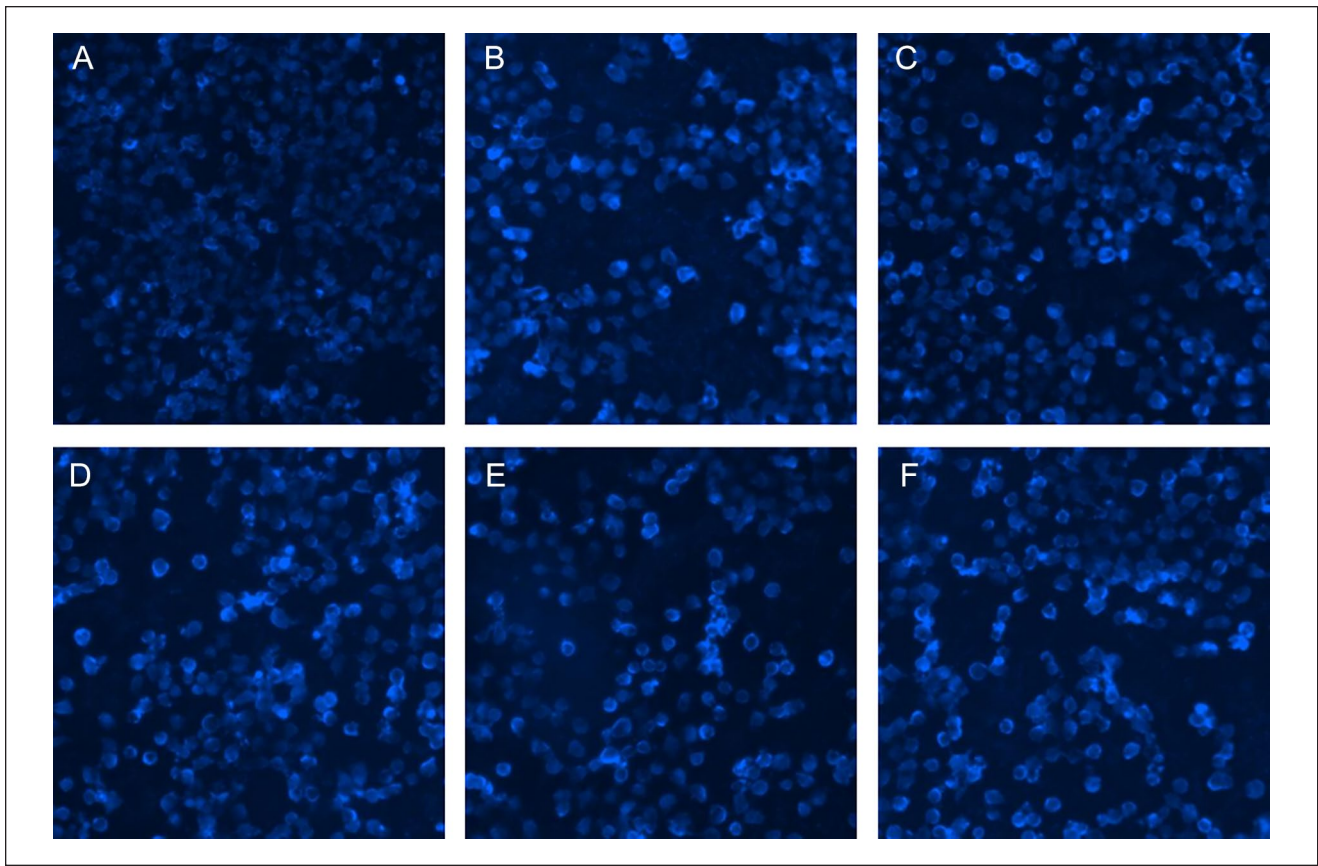


Figure 3. A549 cells were treated with different methods for 48 hours. The cells were stained with Hoechst33258 and images were captured by using an inverted fluorescence microscope. There were shrunken, hyperchromatic, and pyknotic cells and fragmented nuclei in experimental groups. ($\times 10$) (A) Control group. (B) 3W hGAG group. (C) 5W hGAG group. (D) HPD-PDT group. (E) 3W hGAG + HPD-PDT group. (F) 5W hGAG + HPD-PDT group.

Table 2. The Apoptosis Rates of A549 Cells in Different Groups (Mean \pm SD, n=3).

Groups	A (%)	B (%)	C (%)
Control	3.447 \pm 0.239	2.733 \pm 0.127	6.179 \pm 0.374
3W hGAG**	2.868 \pm 1.201	9.915 \pm 1.288	12.783 \pm 1.786
5W hGAG*	4.162 \pm 1.276	6.673 \pm 1.479	10.834 \pm 2.897
HPD-PDT*	4.581 \pm 1.314	10.143 \pm 1.499	14.994 \pm 1.326
3W hGAG + HPD-PDT***	22.583 \pm 5.742	11.828 \pm 3.637	34.410 \pm 5.761
5W hGAG + HPD-PDT**	14.475 \pm 2.907	12.755 \pm 2.306	27.231 \pm 3.366
F value			93.248
P value			<.05

Abbreviations: A, early apoptosis rate; B, late apoptosis rate; C, total apoptosis rate; hGAG, holothurian glycosaminoglycan; HPD-PDT, hemoporphyrin derivative-photodynamic therapy.

* $P < .05$ compared with the control group.

** $P < .05$ compared with the 5W hGAG group.

*** $P < .05$ compared with the HPD-PDT group.

**** $P < .05$ compared with 5W hGAG + HPD-PDT group. The total apoptotic rate was most obvious in 3W hGAG + HPD-PDT group. $P < .05$ was considered statistically significant.

better improve the prognosis of patients at present. But its side effects also need to be paid attention to, such as damage to the immune system and destruction of normal organ

functions.²⁸ In recent years, target therapy and immune therapy have better effects on some patients with particular oncogenic drivers and PD-L1 expression, but drug

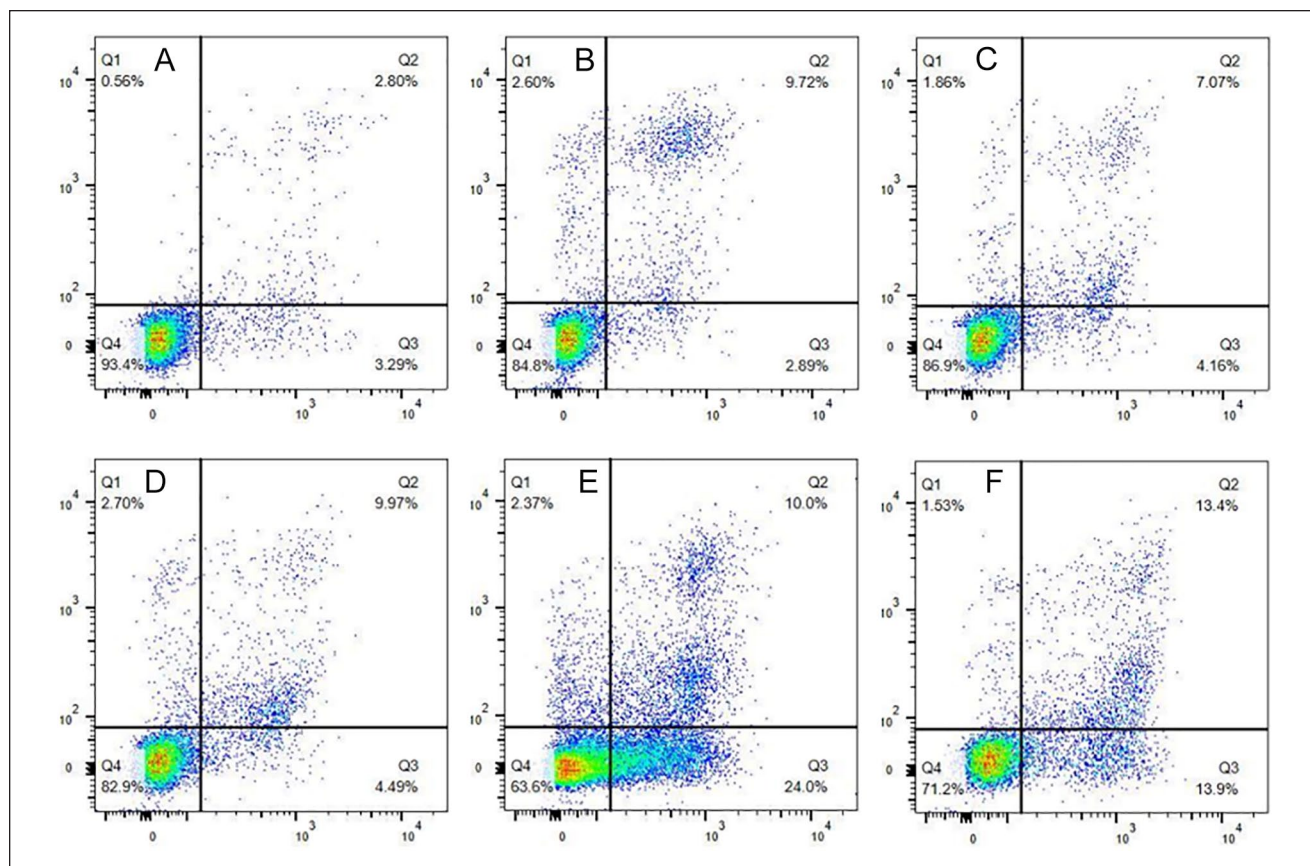


Figure 4. A549 cells were treated with different methods for 48 hours. AnnexinV-FITC/PI double staining was used to distinguish early and late apoptotic cells. The proportion of apoptotic cells was measured by flow cytometry. (A) Control group. (B) 3W hGAG group. (C) 5W hGAG group. (D) HPD-PDT group. (E) 3W hGAG + HPD-PDT group. (F) 5W hGAG + HPD-PDT group.

resistance limits their application in lung cancer treatment.²⁹ Therefore, exploring new treatments and new active components with antitumor effects is essential.

HGAG is an active component extracted from the body wall of sea cucumber in recent years, and cannot be synthesized artificially at present. In previous studies, hGAG has been shown to have antitumor effects, the mechanism for which includes anti-angiogenesis, heparanase activity inhibition, suppressing cell adhesion to platelet-coated surface, regulation of immunoreactivities, cell cycle inhibition, and induction of apoptosis,^{12,30-32} and hGAG can strengthen the sensitivity of tumor cells to chemotherapy.¹⁹ Nowadays, more kinds of low molecular weight hGAG are obtained and their structure-bioactivities are becoming a focus of current studies. There is a close correlation between bioactivities and molecular weight. Some studies have proved that low molecular weight hGAG, as a depolymerized product, demonstrated the same bioactivities as naïve hGAG, such as anti coagulation and hematopoiesis-stimulation.^{11,33} Furthermore, lower molecular weight hGAG can dramatically improve the immune regulation activity.¹⁰ In this study, low molecular weight sea cucumber polysaccharide was obtained by chemical degradation of high molecular

weight sea cucumber polysaccharide. Through the assay of cell proliferative activity and apoptosis rates, the results indicated that the inhibitory effects on A549 cells of 3W molecular weight hGAG was superior to 5W molecular weight hGAG, which also pointed out the direction for further exploring the anti tumor effects of lower molecular weight.

In recent years, as a potential and non-invasive treatment, photodynamic therapy (PDT) is gradually used for the treatment of lung carcinoma. The antitumor mechanisms of PDT include inducing tumor cell necrosis, apoptosis and autophagy, regulating immune response, and destroying tumor nutrient vessels.³⁴⁻³⁹ Because of the capability of normal tissues to clear or eliminate the photosensitizers, the photochemical reaction almost occurs in pathological tissues, and there are almost no phototoxic effects in surrounding normal tissues.³⁷ Compared with conventional treatments, PDT has the advantages of less trauma, less toxicity, repeatability, and high selectivity. With the development of endoscopic technology, PDT is broadly applied in many kinds of tumors, including benign tumors and malignant tumors. Moreover, combination with some novel technologies, such as nanotechnology,

liposome and lipoprotein, and electroporation provides the possibility for improving the efficacy of PDT.⁴⁰ Besides the above aspects, finding out some new components to maximize the efficacy of PDT as far as possible is also a promising direction for lung cancer treatment.

However, due to the limitation on the experimental conditions, this study was only performed on A549 human lung adenocarcinoma cells. It is needed to further investigate the effects of the 2 different molecular weights hGAG on other cell lines and animals. Furthermore, based on our previous study, the mechanism of the sensitization enhancement of hGAG to chemotherapy may correlate with low expression of survivin and Bcl-2 mRNA and protein and high expression of Bax and caspase-3 mRNA and protein.¹⁹ The signaling pathway of the anti tumor effects and immunostimulatory effects is possibly related to suppression of the activation of the ERK1/2/p38 and MAPK/NF- κ B pathway.^{12,18} The mechanism and signaling pathway of the sensitization enhancement of hGAG to HPD-PDT need further elucidation. We speculate that the mechanism of hGAG combined with HPD-PDT on apoptosis may be also associated with the above mechanism. And we will explore protein and gene expressions as well as signaling pathways to validate our speculation in our following experiments. Because of the limitations of separation and purification techniques, only 3W and 5W molecular weights hGAG can be obtained by us, and it is also essential to separate and purify lower molecular weight hGAG, and reveal the inhibitory effects of more kinds of lower molecular weights hGAG combined with HPD-PDT to find appropriate molecular weight hGAG for improvement in HPD-PDT. It is believed that in the future hGAG will become a promising candidate in lung cancer treatment and contribute to the clinical application of HPD-PDT, which brings more benefits to clinicians and lung cancer patients.

Conclusion

In conclusion, 3W and 5W molecular weights hGAG, whether in combination with HPD-PDT or not can cause proliferation inhibition of A549 cells and promote apoptosis rates of A549 cells, which can enhance the sensitivity of A549 cells to HPD-PDT. The combined use of hGAG and HPD-PDT has synergistic effects and the inhibitory effect of 3W molecular weight hGAG is better than that of 5W molecular weight hGAG, which indicates that this synergistic effect may be associated with the molecular weight of hGAG.

Declaration of Conflicting Interests

The author(s) declared no potential conflicts of interest with respect to the research, authorship, and/or publication of this article.

Funding

The author(s) disclosed receipt of the following financial support for the research, authorship, and/or publication of this article: This

project was supported by the Key Laboratory of Marine Drug, Ministry of Education (KLMDOUC201307).

ORCID iD

Dai Hao-Yu  <https://orcid.org/0000-0001-8598-486X>

References

1. Sung H, Ferlay J, Siegel RL. Global cancer statistics 2020: GLOBOCAN estimates of incidence and mortality worldwide for 36 cancers in 185 countries. *CA: Cancer J Clin.* 2021;71:209-249. Doi:10.3322/caac.21660
2. Allemani C, Matsuda T, Di Carlo V, et al. Global surveillance of trends in cancer survival 2000-14 (CONCORD-3): analysis of individual records for 37 513 025 patients diagnosed with one of 18 cancers from 322 population-based registries in 71 countries. *Lancet.* 2018;391:1023-1075. Doi:10.1016/s0140-6736(17)33326-3
3. Chen W, Zheng R, Baade PD, et al. Cancer statistics in China, 2015. *CA: Cancer J Clin.* 2016;66:115-32. Doi:10.3322/caac.21338
4. Zhang X, Liu S, Liu Y, et al. Economic burden for lung cancer survivors in urban China. *Int J Environ Res Public Health.* 2017;14:308. Doi:10.3390/ijerph14030308
5. Cao W, Chen HD, Yu YW, Li N, Chen WQ. Changing profiles of cancer burden worldwide and in China: a secondary analysis of the global cancer statistics 2020. *Chin Med J (Engl).* 2021;134:783-791. Doi:10.1097/cm9.0000000000001474
6. Scrima M, Zito Marino F, Oliveira DM, et al. Aberrant signaling through the HER2-ERK1/2 pathway is predictive of reduced disease-free and overall survival in early stage non-small cell lung cancer (NSCLC) patients. *J Cancer.* 2017;8:227-239. Doi:10.7150/jca.17093
7. Wang X, Cao L, Li S, Wang F, Huang D, Jiang R. Combination of PD-L1 expression and NLR as prognostic marker in patients with surgically resected non-small cell lung cancer. *J Cancer.* 2019;10:6703-6710. doi:10.7150/jca.34469
8. Shi J, Hua X, Zhu B, Ravichandran S. Somatic genomics and clinical features of lung adenocarcinoma: a retrospective study. *PLoS Med.* 2016;13:e1002162. doi:10.1371/journal.pmed.1002162
9. Hossain A, Dave D, Shahidi F. Northern sea cucumber (*Cucumaria frondosa*): a potential candidate for functional food, nutraceutical, and pharmaceutical sector. *Mar Drugs.* 2020;18:274. doi:10.3390/md18050274
10. Gong PX, Wu YC, Chen X, et al. Immunological effect of fucosylated chondroitin sulfate and its oligomers from *Holothuria fuscogilva* on RAW 264.7 cells. *Carbohydr Polym.* 2022;287:119362. doi:10.1016/j.carbpol.2022.119362
11. Li S, Zhong W, Pan Y, et al. Structural characterization and anticoagulant analysis of the novel branched fucosylated glycosaminoglycan from sea cucumber *Holothuria nobilis*. *Carbohydr Polym.* 2021;269:118290. doi:10.1016/j.carbpol.2021.118290
12. Liu X, Liu Y, Hao J, et al. In vivo anti-cancer mechanism of low-molecular-weight fucosylated chondroitin sulfate (LFCS) from sea cucumber *Cucumaria frondosa*. *Molecules.* 2016;21:625. doi:10.3390/molecules21050625

13. Zheng W, Zhou L, Lin L, Cai Y, Sun H, Zhao L. Physicochemical characteristics and anticoagulant activities of the polysaccharides from sea cucumber *Pattalus mollis*. *Mar Drugs*. 2019;17:198. doi:10.3390/md17040198
14. Zhou L, Gao N, Sun H, et al. Effects of native fucosylated glycosaminoglycan, its depolymerized derivatives on intrinsic factor Xase, coagulation, thrombosis, and hemorrhagic risk. *Thrombo Haemost*. 2020;120:607-619. doi:10.1055/s-0040-1708480
15. Hu S, Wang J, Xu Y, et al. Anti-inflammation effects of fucosylated chondroitin sulphate from *Acaudina molpadioides* by altering gut microbiota in obese mice. *Food Funct*. 2019;10:1736-1746. doi:10.1039/c8fo02364f
16. Gong PX, Li QY, Wu YC, Lu WY, Zeng J, Li HJ. Structural elucidation and antidiabetic activity of fucosylated chondroitin sulfate from sea cucumber *Stichopus japonicus*. *Carbohydr Polym*. 2021;262:117969. doi:10.1016/j.carbpol.2021.117969
17. Dwivedi R, Samanta P, Sharma P, et al. Structural and kinetic analyses of holothurian sulfated glycans suggest potential treatment for SARS-CoV-2 infection. *J Biol Chem*. 2021;297:101207. doi:10.1016/j.jbc.2021.101207
18. Wang H, Xu L, Yu M, et al. Glycosaminoglycan from *Apostichopus japonicus* induces immunomodulatory activity in cyclophosphamide-treated mice and in macrophages. *Int J Biol Macromol*. 2019;130:229-237. doi:10.1016/j.ijbiomac.2019.02.093
19. Lin C, Zhu X, Jin Q, Sui A, Li J, Shen L. Effects of holothurian glycosaminoglycan on the sensitivity of lung cancer to chemotherapy. *Integr Cancer Ther*. 2020;19:1-10. doi:10.1177/1534735420911430
20. Allison RR, Moghissi K. Photodynamic therapy (PDT): PDT mechanisms. *Clin Endosc*. 2013;46:24-29. doi:10.5946/ce.2013.46.1.24
21. Abrahamse H, Hamblin MR. New photosensitizers for photodynamic therapy. *Biochem J*. 2016;473:347-364. doi:10.1042/bj20150942
22. Wang M, Song J. NIR-triggered phototherapy and immunotherapy via an antigen-capturing nanoplatfor for metastatic cancer treatment. *Adv Sci*. 2019;6:1802157. doi:10.1002/advs.201802157
23. Luo D, Carter KA, Miranda D, Lovell JF. Chemophototherapy: an emerging treatment option for solid tumors. *Adv Sci*. 2017;4:1600106. doi:10.1002/advs.201600106
24. Gallagher-Colombo SM, Miller J, Cengel KA, Putt ME, Vinogradov SA, Busch TM. Erlotinib pretreatment improves photodynamic therapy of non-small cell lung carcinoma xenografts via multiple mechanisms. *Cancer Res*. 2015;75:3118-3126. doi:10.1158/0008-5472.can-14-3304
25. Qiu H, Cao S, Xu R. Cancer incidence, mortality, and burden in China: a time-trend analysis and comparison with the United States and United Kingdom based on the global epidemiological data released in 2020. *Cancer Commun*. 2021;41:1037-1048. doi:10.1002/cac2.12197
26. Li N, Tan F, Chen W, et al. One-off low-dose CT for lung cancer screening in China: a multicentre, population-based, prospective cohort study. *Lancet Respir Med*. 2022;10:378-391. doi:10.1016/s2213-2600(21)00560-9
27. Thai AA, Solomon BJ, Sequist LV, Gainor JF, Heist RS. Lung cancer. *Lancet*. 2021;398:535-554. doi:10.1016/s0140-6736(21)00312-3
28. Zhang LX, Sun XM, Xu ZP. Development of multifunctional clay-based nanomedicine for elimination of primary invasive breast cancer and prevention of its lung metastasis and distant inoculation. *ACS Appl Mater Interfaces*. 2019;11:35566-35576. doi:10.1021/acsami.9b11746
29. Awad MM, Liu S, Rybkin, II, et al. Acquired resistance to KRAS(G12C) inhibition in cancer. *N Engl J Med*. 2021;384:2382-2393. doi:10.1056/NEJMoa2105281
30. Zhou L, Yin R, Gao N, et al. Oligosaccharides from fucosylated glycosaminoglycan prevent breast cancer metastasis in mice by inhibiting heparanase activity and angiogenesis. *Pharmacol Res*. 2021;166:105527. doi:10.1016/j.phrs.2021.105527
31. Ustyuzhanina NE, Bilan MI, Dmitrenok AS, et al. Fucosylated chondroitin sulfate from the sea cucumber *Hemiodema spectabilis*: structure and influence on cell adhesion and tubulogenesis. *Carbohydr Polym*. 2020;234:115895. doi:10.1016/j.carbpol.2020.115895
32. Yang D, Lin F, Huang Y, Ye J, Xiao M. Separation, purification, structural analysis and immune-enhancing activity of sulfated polysaccharide isolated from sea cucumber viscera. *Int J Biol Macromol*. 2020;155:1003-1018. doi:10.1016/j.ijbiomac.2019.11.064
33. Ustyuzhanina NE, Bilan MI, Anisimova NY, et al. Depolymerization of a fucosylated chondroitin sulfate from *Cucumaria japonica*: structure and activity of the product. *Carbohydr Polym*. 2022;281:119072. doi:10.1016/j.carbpol.2021.119072
34. Rothe F, Patties I. Immunomodulatory effects by photodynamic treatment of glioblastoma cells in vitro. *Molecules*. 2022;27:3384. doi:10.3390/molecules27113384
35. Abo-Zeid MAM, Abo-Elfadl MT, Mostafa SM. Photodynamic therapy using 5-aminolevulinic acid triggered DNA damage of adenocarcinoma breast cancer and hepatocellular carcinoma cell lines. *Photodiagnosis Photodyn Ther*. 2018;21:351-356. doi:10.1016/j.pdpdt.2018.01.011
36. Beltrán Hernández I, Yu Y, Ossendorp F, Korbelik M, Oliveira S. Preclinical and clinical evidence of immune responses triggered in oncologic photodynamic therapy: clinical recommendations. *J Clin Med*. 2020;9:333. doi:10.3390/jcm9020333
37. van Straten D, Mashayekhi V, de Bruijn HS, Oliveira S, Robinson DJ. Oncologic photodynamic therapy: basic principles, current clinical status and future directions. *Cancers*. 2017;9:19. doi:10.3390/cancers9020019
38. Huang Q, Ou YS, Tao Y, Yin H, Tu PH. Apoptosis and autophagy induced by pyropheophorbide- α methyl ester-mediated photodynamic therapy in human osteosarcoma MG-63 cells. *Apoptosis*. 2016;21:749-60. doi:10.1007/s10495-016-1243-4
39. Ouyang G, Xiong L, Liu Z, et al. Inhibition of autophagy potentiates the apoptosis-inducing effects of photodynamic therapy on human colon cancer cells. *Photodiagnosis Photodyn Ther*. 2018;21:396-403. doi:10.1016/j.pdpdt.2018.01.010
40. Kwiatkowski S, Knap B, Przystupski D, et al. Photodynamic therapy - mechanisms, photosensitizers and combinations. *Biomed Pharmacother*. 2018;106:1098-1107. doi:10.1016/j.biopha.2018.07.049